ChemComm

RSC Publishing

COMMUNICATION

View Article Online
View Journal | View Issue

Cite this: *Chem. Commun.*, 2013, **49**, 3772

Received 31st January 2013,
Accepted 21st March 2013

DOI: 10.1039/c3cc40836a

www.rsc.org/chemcomm

Polysaccharide-lecithin reverse micelles with enzyme-degradable triglyceride shell for overcoming tumor multidrug resistance†

Chia-Wei Su, San-Yuan Chen* and Dean-Mo Liu*

A newly-designed drug carrier with enzyme-triggered release behavior and the ability to circumvent multidrug resistance was successfully developed. By optimizing the ratio of lecithin and polysaccharide in reverse micelles, encapsulation efficiency and encapsulation stability can be significantly improved.

Chitosan, a polysaccharide derived from the deacetylation of chitin, is well-known to exhibit superior biocompatibility and bioadhesivity[1] and subsequently numerous chitosan-based drug carriers have been developed.[2] However, poorly controlled drug release and physical stability still hinder their further applications. Recently, enzyme-responsive drug delivery systems have attracted more interest because the enzymes exist only in specific areas such as disease sites[3] and intracellular vesicles,[4] and thus endow selective catalytic action to trigger drug release. Moreover, triglyceride, an enzyme-degradable material, is well known to provide desired characteristics, including physical stability, capability of protecting labile drugs from degradation,[5] and especially the ability to overcome multidrug resistance,[6] which has not been achievable through the use of chitosan-based derivatives. Multidrug resistance (MDR) is mediated by drug resistance efflux pumps (P-glycoprotein, P-gp) on the cell membrane and has been found in various types of cancer cells, which results in the failure of chemotherapeutic treatment.[7] For this reason, the collaboration of micelle and triglyceride nanoparticle systems is a prospective design for novel chemotherapeutic formulation.

In this study, a newly-designed drug carrier (termed D-PL/TG NPs) that is composed of drug-loaded polysaccharide–lecithin reverse micelles and a triglyceride shell on the exterior has been developed by an ultrasonic emulsification and solvent evaporation process, as depicted in Scheme 1. We used a conceptually different approach to encapsulate DOX within the inner aqueous phase of reverse micelles, so that the encapsulation efficiency can be well improved *via* this process. DOX as a model drug was chosen because it is one of the most effective and widely used anticancer substances; however its potency is seriously undermined by MDR.[7] Amphiphilic carboxymethyl-hexanoyl chitosan (CHC, chemical structure shown in Fig. S1a, ESI†) was developed in this lab[8] and used as the constituent of reverse micelles. The pre-dissolved DOX and CHC solution was first added to an organic solution containing lecithin and glycerol tripalmitate. After the first-step water-in-oil (w/o) emulsification, polysaccharide-lecithin reverse micelles with encapsulated DOX were formed and distributed in the organic phase. The CHC acted as a physical barrier to encapsulate DOX and reduce its leakage during synthesis. Lecithin was utilized to improve the stability of the reverse micelles in the organic phase. An oil emulsion containing reverse micelles was emulsified with sodium cholate in the aqueous phase after the second-step oil-in-water (o/w) emulsification. The resulting doxorubicin-loaded nanoparticles were subsequently obtained after removing the organic solvent by evaporation.

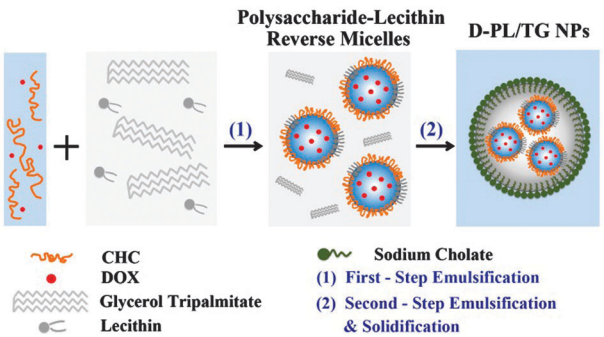

Scheme 1 Synthesis procedure of D-PL/TG NPs.

The character of the DOX-loaded polysaccharide–lecithin reverse micelles (termed D-PL RMs) was analyzed by Fourier

Department of Materials Sciences and Engineering, National Chiao Tung University, Hsinchu, 30010, Taiwan. E-mail: sanyuanchen@mail.nctu.edu.tw, deanmo_liu@yahoo.ca; Fax: +886-3-5724727; Tel: +886-3-5712121, ext. 31818; ext. 55391

† Electronic supplementary information (ESI) available: Experimental details, characterization by XRD, DSC, and SAXS and fluorescent images. See DOI: 10.1039/c3cc40836a

transform infrared spectroscopy (FTIR) spectra (Fig. S1b, ESI†) and TEM (Fig. S1c, ESI†). Table S1 (ESI†) provides the mean sizes, PDI values and zeta potentials of the D-PL/TG NPs with various compositions. The size of the D-PL/TG NPs slightly increased from 161.7 nm to 181.4 nm as the CHC ratio increased from 0 to 40%; the zeta potentials of these D-PL/TG NPs are all close to −30 mV, showing that they have good physical stability in solution. To confirm the existence of a triglyceride shell coating on the exterior of the reverse micelles, the differences in structural development of the nanoparticles, GT (bulk triglyceride), TNPs (triglyceride nanoparticles), PL/TG NPs (reverse micelles with triglyceride shell, but DOX-free) and D-PL/TG NPs (DOX-loaded reverse micelles with triglyceride shell) were analyzed using differential scanning calorimetry (DSC) and X-ray diffraction (XRD). The DSC spectra of the nanoparticles along with their constituents are presented in Fig. 1a and Table S2 (ESI†). The TNPs melted between 54.29 and 63.99 °C with the melting peak at 61.63 °C, but the melting peak of PL/TG NPs decreased by 3.4 °C. The depression of the melting point suggested a less-ordered arrangement of the triglyceride molecules in PL/TG NPs, which was supposed to be induced by the encapsulation of the reverse micelles in the areas of crystal imperfections. Moreover, melting peaks of PL/TG NPs and D-PL/TG NPs are preceded by endothermic shoulders (arrows in Fig. 1a), which originate from the melting of poor crystalline fractions.[9]

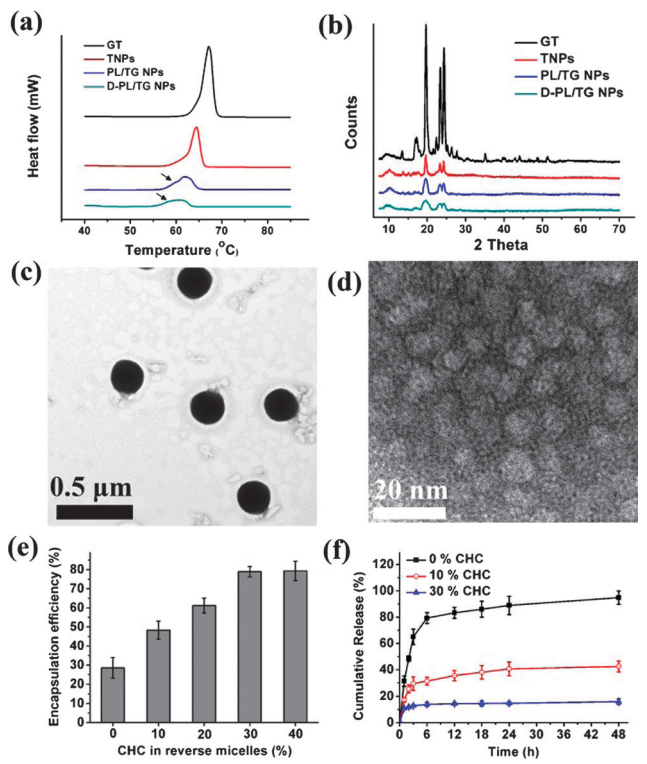

Fig. 1 (a) DSC spectra and (b) X-ray diffraction patterns of the designed nanoparticles. (c) Micrograph of D-PL/TG NPs with 30% CHC by transmission electron microscopy. (d) Localized region under high magnification. (e) Encapsulation efficiencies of designed D-PL/TG NPs (shown in Table S1, ESI†). (f) *In vitro* drug release study of D-PL/TG NPs with 0%, 10% and 30% CHC in pH 7.4 phosphate buffer at 37 °C (measured in triplicate).

The characterized peaks of the XRD patterns demonstrate that the tripalmitate in all conditions is arranged with β-phase order (Fig. 1b).[9] The reduction in the peak intensity of the XRD patterns suggests that the encapsulation of reverse micelles further deteriorates the crystalline structure of the triglyceride shell. (Fig. S2, ESI†). Consequently, the results of the DSC and XRD measurements confirm that triglyceride shells have been successfully coated onto the exteriors of the reverse micelles.

A TEM micrograph (Fig. 1c) shows that the D-PL/TG NPs exhibit spherical shape with a uniform size. The magnified TEM image reveals that polysaccharide–lecithin reverse micelles became numerous pores distributed within the nanoparticles after the inner aqueous phase was removed (*via* evaporation), as shown in Fig. 1d. In addition, the pore size of the D-PL/TG NPs with 30% CHC is greater than that of the D-PL/TG NPs with 10% CHC (Fig. S2a, ESI†), which was confirmed by small angle X-ray scattering (SAXS, Fig. S2b, ESI†) measurements. This can be explained by the fact that larger reverse micelles evolved on increasing the CHC ratio. The encapsulation efficiencies of the prepared D-PL/TG NPs are shown in Fig. 1e. A significantly improved encapsulation efficiency can be achieved from 29% to 80%, demonstrating that the physical barrier provided by CHC and the triglyceride shell was evidenced in improving the encapsulation efficiency of the nanocarrier. However, a further increase in the CHC ratio to 40% resulted in no improvement in encapsulation efficiency, which was likely due to a decrease in the solubility of DOX at high CHC concentrations in the aqueous phase. Therefore, focus was directed toward the use of D-PL/TG NPs-3 because they exhibited the most optimal drug carrying efficiency among other parameters. The *in vitro* release profiles of the D-PL/TG NPs exhibit a two-stage pattern over a 48 h release test, as shown in Fig. 1f, where a burst release is observed in the first 6 h, followed by a slow release over a prolonged period of an additional 42 h. Encapsulation stability is an important issue for drug carriers to minimize accidental leakage.[10] The reduction of total release amount indicated that the encapsulation stability of the drug carrier was significantly improved as the CHC ratio increased.

To evaluate the degradation behavior of the triglyceride shell and the release of DOX, we performed kinetic studies in a simulated lysosomal environment. Fig. 2a–d present TEM images of D-PL/TG NPs stored in a simulated lysosomal environment for 72 h. After 24 h storage, the peripheries of the nanoparticles appeared as luna-like gray areas, indicating that lysosomal acid lipase (LAL) had began to degrade the

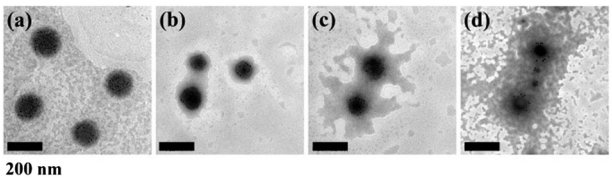

Fig. 2 Kinetic studies of triglyceride degradation by the environment for (a) 0 h, (b) 24 h, (c) 48 h and (d) 72 h.

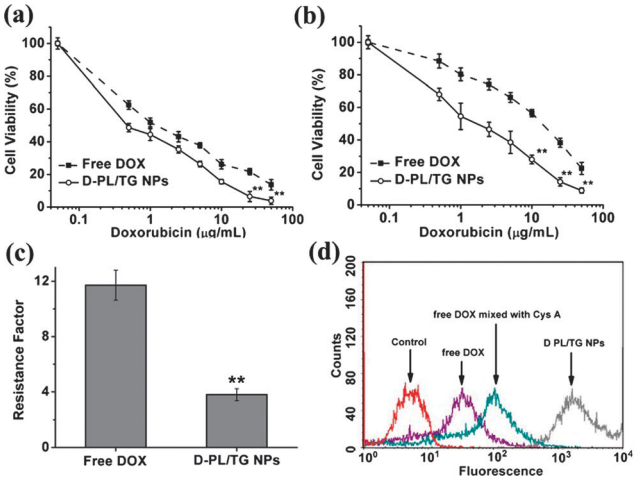

Fig. 3 *In vitro* cytotoxicity of free DOX and D-PL/TG NPs against MCF-7 cells (a) and MCF-7/ADR cells (b), respectively. $^{**}p < 0.01$ and $^{*}p < 0.05$ compared with free DOX. (c) Resistance factor obtained from the viability assay ($^{**}p < 0.01$). (d) The fluorescence intensities of MCF-7/ADR cells after 4 h incubation with free DOX, free DOX mixed with Cys A and D-PL/TG NPs were detected by flow cytometry.

nanoparticles from their outer lipid shell. The gray areas displayed an irregular shape after 48 h storage and were accompanied by several small fragments, which were supposed to be the triglyceride components of D-PL/TG NPs. After 72 h storage, the peripheral gray areas were greater in size than the central black areas and were more irregular, suggesting that the majority of each triglyceride shell had degraded. Hydrolysis of the triglyceride shells and release of encapsulated DOX in D-PL/TG NPs were demonstrated to be significantly triggered by LAL.

The endocytic pathway of D-PL/TG NPs was examined by incubating MCF-7 cells with several specific endocytic inhibitors. Their fluorescence intensity from internalized DOX was measured by flow cytometry and the subcellular localization of the internalized nanoparticles was visualized by confocal microscopy. As shown in Fig. S4 (ESI†), the results confirm that D-PL/TG NPs were delivered into lysosomes and subsequently the triglyceride shell was degraded by LAL to release the drug intracellularlly.[11]

To evaluate the ability of the D-PL/TG NPs to circumvent P-gp mediated multidrug resistance, we investigated the viability of MCF-7 and MCF-7/ADR cells using an MTT method. After incubating with a series of equivalent concentrations of free DOX or D-PL/TG NPs for 72 h, the IC_{50} values of free DOX and D-PL/TG NPs against MCF-7 cells were determined to be 1.31 ± 0.02 μg mL^{-1} and 0.49 ± 0.03 μg mL^{-1}, respectively (Fig. 3a and b). D-PL/TG NPs exhibited greater cytotoxicity, which is likely due to uptake of the nanoparticles with considerable amounts of encapsulated DOX and consequent higher accumulated intracellular concentration. In contrast, free DOX lacked the controlled release to achieve effective intracellular concentration to inhibit the viability of MCF-7 cells. The IC_{50} values of free DOX and D-PL/TG NPs against MCF-7/ADR cells were 15.38 ± 0.15 μg mL^{-1} and 1.85 ± 0.05 μg mL^{-1}, respectively, which demonstrates that P-gp overexpression in MCF-7/ADR cells impeded the cytotoxicity of free DOX more than that of D-PL/TG NPs. These trends of drug response are more clearly observed by comparing the ratios of the IC_{50} values obtained from the viability assay. As shown in Fig. 3c, the resistance factor (*i.e.*, the ratio of IC_{50} values) of free DOX was 11.72 ± 1.53, but that of the D-PL/TG NPs was only 3.81 ± 0.84. A significantly improved cytotoxicity can be obtained by encapsulating DOX into PL/TG NPs, and the prevention of drug efflux from drug-resistant cells can thus be achieved. Further evidence for the ability of D-PL/TG NPs to circumvent drug efflux-mediated resistance is the uptake amount of DOX by the cells. The fluorescence emission from inside MCF-7/ADR cells after 4 h incubation with free DOX, free DOX mixed with Cys A and D-PL/TG NPs was determined using flow cytometry. The uptake amount of DOX on D-PL/TG NPs treatment was greater than that on treatment with free DOX, which is consistent with D-PL/TG NPs being more cytotoxic against MCF-7/ADR cells than the free drug. It is noteworthy that in the presence of Cys A (10 μg mL^{-1}), a known inhibitor of P-gp, a greater uptake of DOX by the cells was detected than that on treatment with free DOX, whereas the amount was still lower than that on D-PL/TG NPs treatment. Free DOX was internalized into the MCF-7/ADR cells by diffusion, which was easily captured and excluded by P-gp. In contrast, the D-PL/TG NPs can circumvent P-gp mediated multidrug resistance by internalizing the carriers through endocytosis, corresponding to enhanced intracellular accumulation and cellular cytotoxicity.

A newly-designed drug carrier was successfully developed, which represents an advanced paradigm for the collaboration of micelle and polymeric nanoparticle systems.

Notes and references

1 A. Fini and I. Orienti, *Am. J. Drug Delivery*, 2003, **1**, 43–59.
2 B. Hu, Y. W. Ting, X. Q. Yang, W. P. Tang, X. X. Zeng and Q. R. Huang, *Chem. Commun.*, 2012, **48**, 2421–2423.
3 C. Park, H. Kim, S. Kim and C. Kim, *J. Am. Chem. Soc.*, 2009, **131**, 16614–16615.
4 L. A. Bareford and P. W. Swaan, *Adv. Drug Delivery Rev.*, 2007, **59**, 748–758.
5 W. Mehnert and K. Mader, *Adv. Drug Delivery Rev.*, 2001, **47**, 165–196.
6 H. L. Wong, R. Bendayan, A. M. Rauth, Y. Q. Li and X. Y. Wu, *Adv. Drug Delivery Rev.*, 2007, **59**, 491–504.
7 M. F. Fromm, *Adv. Drug Delivery Rev.*, 2002, **54**, 1295–1310.
8 K. H. Liu, S. Y. Chen, D. M. Liu and T. Y. Liu, *Macromolecules*, 2008, **41**, 6511–6516.
9 M. Kellens, W. Meeussen and H. Reynaers, *Chem. Phys. Lipids*, 1990, **55**, 163–178.
10 R. T. Chacko, J. Ventura, J. M. Zhuang and S. Thayumanavan, *Adv. Drug Delivery Rev.*, 2012, **64**, 836–851.
11 T. G. Iversen, T. Skotland and K. Sandvig, *Nano Today*, 2011, **6**, 176–185.

